

UHMWPE-Layered Silicate Nanocomposites by *in situ* Polymerization with Tris(pyrazolyl)borate Titanium/Clay Catalyst

Fernando Junges,^a Mariana S. Beauvalet,^a Bárbara C. Leal,^a Adriana C. A. Casagrande,^a
Fábio F. Mota,^b Raquel S. Mauler^a and Osvaldo L. Casagrande Jr.^{a,*}

^aInstituto de Química, Universidade Federal do Rio Grande do Sul, Av. Bento Gonçalves, 9500,
90501-970 Porto Alegre-RS, Brazil

^bCentro de Inovação e Tecnologia Braskem, Via Oeste, Lote 5, Passo Raso, III Pólo Petroquímico,
95853-000 Triunfo-RS, Brazil

Nanocompósitos de polietileno-MMT foram preparados através da metodologia de polimerização *in situ* utilizando $\text{Tp}^{\text{Ms}^*}\text{TiCl}_3$ (**1**) intercalado na galeria da Cloisite® 30B (C30B) e na presença de metilaluminoxano (MAO) como ativador. Através da análise de difração de raios-X (DRX) foi observado que o espaçamento basal da argila ativada muda de 1,85 nm ($2\theta = 4,8$) para 2,18 nm ($2\theta = 4,0$) indicando a ocorrência da intercalação do catalisador de titânio na galeria da argila. O sistema catalítico 1/C30B/MAO foi ativo na polimerização do etileno sob diferentes condições reacionais. A morfologia esfoliada do nanocompósito PE-MMT foi confirmada pela análise de difração de raios-X (DRX) e microscopia eletrônica de transmissão (MET). A presença de argila esfoliada (5% em peso) na matriz polimérica confere melhores propriedades mecânicas (módulo de flexão e módulo de armazenamento) quando comparada com aquelas apresentadas pelo polietileno puro produzido exclusivamente por **1**.

Polyethylene-MMT nanocomposites were prepared by *in situ* polymerization methodology using $\text{Tp}^{\text{Ms}^*}\text{TiCl}_3$ (**1**) intercalated into the gallery of Cloisite® 30B (C30B) using methylaluminoxane (MAO) as activator. From the powder X-ray diffraction (XRD) analysis it was observed that the basal spacing of the activated organoclay changes from 1.85 nm ($2\theta = 4.8$) to 2.18 nm ($2\theta = 4.0$) indicating that the intercalation of the titanium catalyst into the gallery took place. The catalytic system 1/C30B/MAO was active in the ethylene polymerization under different reaction conditions. The exfoliated morphology of the PE-MMT nanocomposite was further examined and confirmed by X-ray diffraction (XRD) and transmission electron microscopy (TEM) analysis. The presence of exfoliated clay (5 wt.%) in the PE matrix confers better mechanical properties (flexural modulus and storage modulus) when compared with the ones displayed by the neat PE produced using exclusively **1**.

Keywords: clay, UHMWPE, nanocomposites, titanium catalyst

Introduction

In recent years, polymer-clay nanocomposites have attracted much academic and industrial interest because of the anticipated improvements in mechanical properties, stiffness, thermal stability, chemical resistance, high barrier properties, flame retardancy, etc. when the aluminosilicate platelets of clays like montmorillonite are well exfoliated into polymers.¹⁻⁴

Several methods have been adopted to prepare polymer-clay nanocomposites, such as self-assembly of exfoliated

inorganic layers with polymers, template synthesis of layered crystals in the polymer solution, melting intercalation, and direct ion exchange of polyelectrolyte with hosts.⁵ More recently, special attention has been devoted to *in situ* intercalative polymerization methodology which is frequently also referred to as “polymerization filling”. In this process, the monomer together with the polymerization initiator or catalyst is intercalated within the silicate layers and the polymerization is initiated either thermally or chemically. In contrast to highly viscous polymer melts, the polymerization reaction media have much smaller viscosity and enable easy dispersion of nanoparticles, provided that the compatibilities of media

*e-mail: osvaldo.casagrande@ufrgs.br

and nanoparticles are matched. Moreover, polymerization filling process can produce nanocomposites with much higher nanofiller content. This strategy has been utilized to produce a variety of economically important polymer-clay nanocomposites based on poly(methyl methacrylate),⁶⁻⁸ polylactide,⁹ polyurethanes,¹⁰ poly(ϵ -caprolactone),^{11,12} and polystyrene.^{7,13-15} Furthermore, this approach has been extremely useful to produce well-exfoliated nanocomposites based on apolar polyolefins in spite of their hydrophobic properties that lack suitable interactions with the polar aluminosilicate surface of the clay. In this case, the vast majority of these studies are concerned to polypropylene,¹⁶⁻²⁰ linear low-density polyethylene,²¹⁻²³ and high-density polyethylene.²⁴⁻³² On the other hand, just one example of ultra high molecular weight polyethylene (UHMWPE)-layered silicate is described in the literature using polymerization filling technique. For instance, Jérôme and co-workers³³ reported the production of UHMWPE nanocomposites by *in situ* intercalative polymerization process using a titanium catalyst $[\text{Me}_2\text{Si}(\text{Me}_4\text{Cp})(\text{N}^i\text{Bu})]\text{TiMe}_2$. Herein, we report the synthesis and characterization of intergallery-anchored $\text{Tp}^{\text{Ms}^*}\text{TiCl}_3$ ($\text{Tp}^{\text{Ms}^*} = \text{HB}(3\text{-mesitylpyrazolyl})_2(5\text{-mesitylpyrazolyl})^-$) into an organophilically modified montmorillonite clay (Cloisite® 30B), by methyl, tallow, bis-2-hydroxyethyl quaternary ammonium chloride (MT_2EtOH), and its application in the production of UHMWPE-layered silicate nanocomposites.

Experimental

Materials

All manipulations were carried out under Ar atmosphere using standard Schlenk tube techniques. $\text{Tp}^{\text{Ms}^*}\text{TiCl}_3$ was synthesized following procedures described in the literature.³⁴ Cloisite® 30B (Southern Clay Products) was dried under vacuum ($P < 10^{-4}$ mbar) for 8 hours at 150 °C. Ethylene (polymer grade), provided by White Martins, and argon were deoxygenated and dried through column of BTS (BASF) and molecular sieve (3A) activated prior to use. MAO (Witco, 5.21 wt.% toluene solution which contains *ca.* 20 wt.% TMA, trimethylaluminum) was used as received. Toluene and hexane were refluxed and distilled over sodium diphenylketyl complex prior to use.

Intercalation procedure of $\text{Tp}^{\text{Ms}^*}\text{TiCl}_3$ into the activated-Cloisite® 30B

A toluene solution of $\text{Tp}^{\text{Ms}^*}\text{TiCl}_3$ (**1**) (0.021 g, 30 μmol) was cannula-transferred into predried Cloisite® 30B (1.0 g)

toluene slurry (20 mL). The reaction mixture was stirred at ambient temperature for 24 h. The slurry was then filtered through a fritted disk. The resulting solid was washed several times (*ca.* 5×10 mL) with toluene at 50 °C, and dried under vacuum for 24 h. The resulting solid was named 1/C30B.

Polymerization procedures

All polymerization reactions were performed in Fisher-Porter reactors (0.1 L or 4 L) equipped with mechanical stirrer. Under ethylene atmosphere, the proper amounts of solvent (toluene or hexane) and MAO were introduced sequentially. After complete thermal equilibration, the slurry solution containing **1** or 1/C30B was added with stirring. The total pressure was kept constant by a continuous feed of ethylene. The polymerization runs were stopped by introducing acidic ethanol. The polymers were washed with acidic ethanol, then ethanol and water, and dried in a vacuum oven at 60 °C for 12h.

Intercalated Ti catalyst and PE-nanocomposite characterization

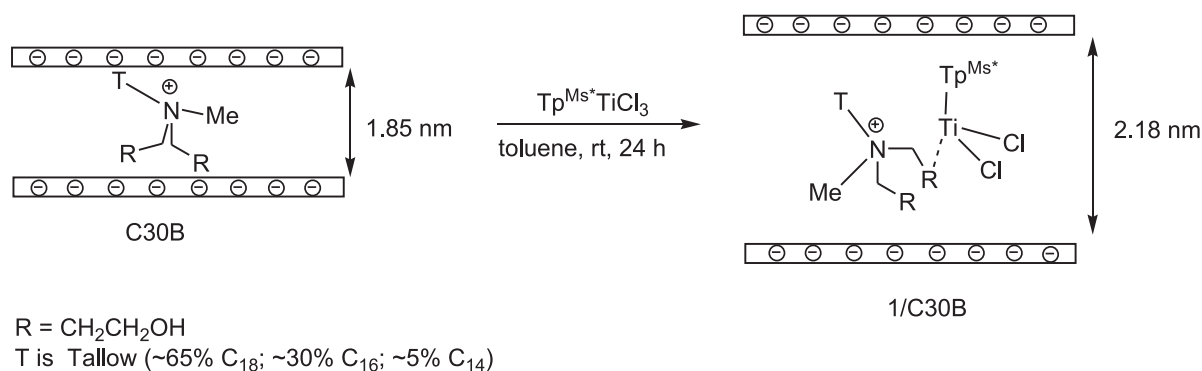
An inductively coupled plasma optical emission (ICP-OES) spectrometer from PerkinElmer (Optima™ 2000 DV) was used for Ti measurement in the clay. A Scott spray chamber and a GemCone® nebulizer composed the sample introduction system. Catalyst digestion was done with H_2SO_4 and HNO_3 ($\text{H}_2\text{SO}_4/\text{HNO}_3$, 3:1) in Teflon® capped vessel. The mixture was heated at 160 °C for 8 h in a heating block (Tecnal, Brazil). Sample and blank were analyzed in duplicate. The intrinsic viscosity of the neat PE and PE-MMT nanocomposite samples were analyzed using in a modified procedure in which the PE was firstly dissolved in decaline (concentrations of 0.02 g dL⁻¹) at 165 °C, filtered through a 0.2 mm filter in order to remove the clay structure and then the PE solution was transferred quickly to a modified Ubelohde viscometer at 135 °C. Based on the experimental intrinsic viscosity values $[\eta]$ it was possible to calculate the viscometric molar mass according to the formula $[\eta] = k(\overline{M}_v)^\alpha$, for $k = 6.7 \times 10^{-4}$ dL g⁻¹ and $\alpha = 0.67$.³⁵ Thermal and crystallization behaviors were determined using Thermal Analysis 2100/TA Instruments. The temperature and energy readings were calibrated with indium and zinc according to ASTM D3417 and D3418. All measurements were carried out in nitrogen atmosphere. The sample was heated to 150 °C, kept at this temperature for 5 min, then cooled and heated at constant rates of 5 °C min⁻¹. Thermogravimetric (TG) was carried out under dried air with a Thermal

Analysis Instruments Q500 Thermogravimetric Analyzer with a heating rate of $10\text{ }^{\circ}\text{C min}^{-1}$ from room temperature to $900\text{ }^{\circ}\text{C}$. The percentage of residual ashes (filler) was taken as the value reported at $600\text{ }^{\circ}\text{C}$. Dynamic Mechanical Thermal Analysis (DMTA) was carried out using a TA Instruments 2980 operating in the tensile mode. The sample dimensions were $0.15\times 7.0\times 12\text{ mm}$. Measurements were taken at 1 Hz . The temperature was raised from -150 to $150\text{ }^{\circ}\text{C}$, at a scanning rate of $2\text{ }^{\circ}\text{C min}^{-1}$. The flexural moduli of the nanocomposites were evaluated using a Universal Test Machine (INSTRON 4204) according to ASTM D-790. The tensile bars (at $23\text{ }^{\circ}\text{C}$) of neat and PE-clay were submitted to a deformation force over two supports, the force was applied at the bar central point at selected displacement rate of 13 mm min^{-1} , the sample dimensions were $13\times 57\times 19\text{ mm}$. Heat Deflection Temperature was measured using a CEAST Vicat Auto machine Model P/N 6970.000 according to ASTM D 648. The sample position was edgewise and surface stress was 0.45 or 1.82 MPa . Silicon oil was used to facilitate the heat transfer; the temperature was registered at 0.25 mm deflection. The X-ray diffractograms were obtained with a Siemens D-500 diffractometer. Films were scanned in the reflection mode using an incident X-ray of Cu K_{α} radiation with wavelength

of 1.542 \AA at a step size of $0.05^{\circ}\text{ min}^{-1}$ from $2\theta = 1^{\circ}$ to 10° . The transmission electronic microscopy analysis was carried out using ultra thin cuts obtained from the compressed specimens in a JEOL JEM-120 EXII TEM microscope operating at an accelerating voltage of 80 kV . The cuts were placed on 300 mesh Cu grids.

Results and Discussion

The organomodified Cloisite[®] 30B (C30B) was selected considering the hydroxyl groups attached to the alkylammonium cations in the clay galleries which can act as the potential binding sites for coordination of the titanium complex.³⁴ Thus, the predried C30B reacted with toluene solution of $\text{Tp}^{\text{Ms}^*}\text{TiCl}_3$ (**1**) for 24 h to generate the intercalated titanium catalyst $1/\text{C30B}$ (Scheme 1). The resulting metal content on the clay determined by ICP-OES was $20\text{ }\mu\text{mol Ti g}^{-1}$ of clay. On the basis of the powder X-ray diffraction (XRD) analysis, it was observed that the basal spacing of the predried C30B changes from 1.85 nm ($2\theta = 4.8$) to 2.18 nm ($2\theta = 4.0$) indicating that the intercalation of the titanium catalyst into the clay gallery took place (Figure 1). In this case, the increased spacing from predried C30B to $1/\text{C30B}$ is consistent with the



Scheme 1

Table 1. Ethylene polymerization results using **1** and $1/\text{C30B}^a$

Entry	T / $^{\circ}\text{C}$	[Al]/[Ti]	time / min	$m_{\text{clay}} / \text{g}$	$m_{\text{pol/clay}} / \text{g}$	activity ^b	$T_c / ^{\circ}\text{C}$	$T_m / ^{\circ}\text{C}$	$\Delta H_m / (\text{mJ mg}^{-1})$	$\chi / (\%)$	clay ^c / (%)
1 ^d	60	500	30	-	1.700	1739	119	136	200	70	-
2	30	500	60	0.103	0.183	40	113	136	117	41	56
3	60	500	60	0.100	0.700	300	116	136	166	58	14
4	80	500	60	0.105	0.499	197	113	137	149	52	21
5 ^{d,e}	60	2500	10	-	184.0	8762	119	135	177	62	-
6 ^e	60	2500	10	6.300	126.0	6000	121	135	189	66	5

^aPolymerization conditions: Fischer Porter bottle (100 mL), [Ti] = $2\text{ }\mu\text{mol}$, toluene = 70 mL ; MAO as cocatalyst, $P_{\text{C}_2\text{H}_4} = 3.0\text{ atm}$; ^bkg of PE/mol[Ti] h; ^cpercentage determined by TGA; ^dethylene polymerization using **1** in homogeneous phase. ^e[Ti] = $126\text{ }\mu\text{mol}$, hexane = 2 L ; MAO as cocatalyst, $P_{\text{C}_2\text{H}_4} = 6.0\text{ atm}$.

molecular dimensions of the titanium catalyst whereas the mesityl groups present in Tp^{Ms} ligand determine significant steric crowding around the TiCl_3 unit.³⁴

The ethylene polymerization behavior of 1/C30B has been evaluated using methylaluminoxane (MAO) as cocatalyst. Representative results are given in Table 1. Initial study carried out at 60 °C with MAO-to-Ti ratio of 500 showed that this catalytic system was possible to polymerize ethylene with activity of 300 kg of PE *per* (mol [Ti] h) (entry 3). As expected, the intercalated catalyst showed lower activity than the one presented by the equivalent homogeneous system (entry 1, 1739 kg of PE *per* (mol [Ti] h)) in consequence of lower amount of potentially available Ti centers present into the clay gallery. However, lower ethylene diffusion into the gallery, which would induce catalyst decay, cannot be ruled out.

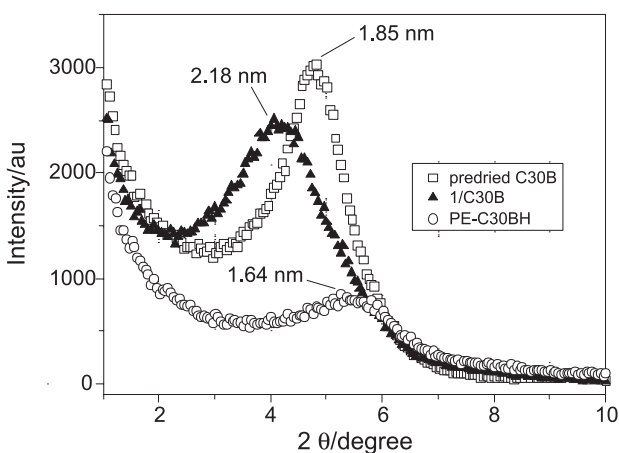


Figure 1. X-ray diffractograms of the activated C30B, 1/C30B and PE-C30BH nanocomposite.

The influence of polymerization temperature on activity has been evaluated in the range of 30–80 °C with MAO-to-Ti ratio of 500. The optimal operating temperature for 1/C30B is 60 °C. At 30 °C, a very low activity was found for this catalytic system, while at 80 °C partial catalyst deactivation was observed.

The melting point (T_m) of the PE-MMT nanocomposites (PE-C30B) was not affected by the presence of clay (136–137 °C). On the other hand, lower crystallization temperatures (T_c) have been found for these polymeric materials in comparison with the neat PE. In addition, for all filled polymers a loss of crystallinity can be detected which is observable in the reduction of ΔH_m (entry 1, *vs* 2–4). It can be supposed that this behavior is due to the presence of higher amounts of clay in the PE matrix (14–56 wt.%) that difficults the crystallization process.

Based on these results, some additional reactions were performed in order to decrease the amount of clay in the

polymeric matrix. For that, the ethylene polymerization reactions were carried out in a 4L Fischer Porter reactor using hexane as solvent at higher ethylene pressure (6 atm).^{36,37} Under these polymerization conditions, the activity for **1** reached 8762 kg of PE *per* mol [Ti] h while the use of 1/C30B displayed an activity of 6000 kg of PE *per* (mol [Ti] h) (entries 5–6). In this case, the lower amount of clay (5 wt.%) incorporated in the PE matrix (PE-C30BH) determined a small impact on the T_m (135 °C) and T_c (121 °C) attaining values very close to those ones of the neat PE. Moreover, for PE-C30BH nanocomposite was observed a slightly increase of crystallinity ($\Delta H_m = 189 \text{ mJ mg}^{-1}$) compared to neat PE ($\Delta H_m = 177 \text{ mJ mg}^{-1}$) which can be associated to the nucleation effect of the MMT on the PE.

The viscosity-average molecular weight (\overline{M}_v) values indicated the formation of ultra high molecular weight PE (UHMWPE); however the presence of clay particles provided a production of PE with lower molecular weight ($2.94 \times 10^6 \text{ g mol}^{-1}$) in comparison with the neat PE ($4.85 \times 10^6 \text{ g mol}^{-1}$). Such results suggest that the presence of well-dispersed clay in the PE matrix can retard the diffusion of ethylene and consequently the probability of chain propagation decreases with the clay loading.^{38,39}

The montmorillonite exfoliation/dispersion within the PE matrix has been analyzed by both XRD and transmission electronic microscopy (TEM). The powder XRD of the PE-C30BH showed the absence of the diffraction peak at $2\theta = 4.8$ indicating the formation of an exfoliated PE-MMT nanocomposite (Figure 1). In addition, the appearance of weak intensity diffraction peak at $2\theta = 5.4$ suggests the occurrence of non exfoliated clay with lower basal spacing (1.64 nm) that can be associated with the presence of natural no modified montmorillonite (MMT-Na).

Transmission electron micrographs of microtomed section of PE-C30BH nanocomposite confirmed homogeneous distribution of clay into the PE matrix as presented in Figure 2. Uniform dispersion is important because if the matrix consists of aggregates of particles, the stress field in the vicinity of the aggregate will be high, resulting in easier crack initiation and propagation, and consequent premature failure. In addition, Figure 2 reveals a good exfoliation of the C30B, with some few multilayer tactoids with expanded layer spacing still remaining.

Overall, their mechanical properties showed some improvements when compared with those ones displayed by the PE produced using exclusively **1**. For instance, for the PE-C30BH it was observed an increase of the flexural modulus from 1050 (neat PE) to 1300 MPa, which is an improvement of 24%. Moreover, it was observed an increase of 10% in the temperature of deflection (HDT,

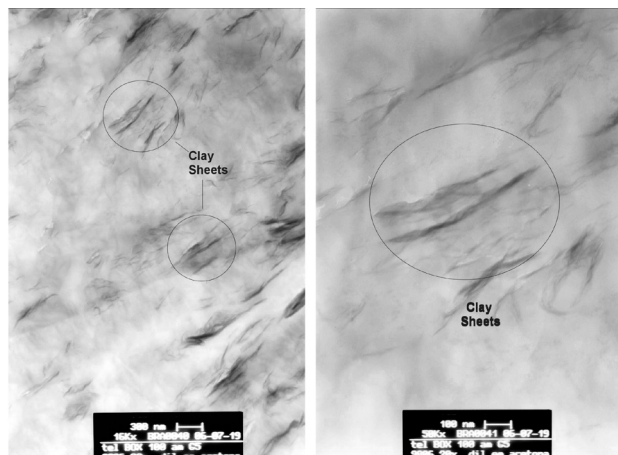


Figure 2. TEM images for a PE-C30BH nanocomposite containing 5 wt.% of organo-modified montmorillonite (entry 6).

from 43 to 48 °C). From DMA results it can be found that the incorporation of C30B increases significantly the storage modulus (E') of PE over the entire temperature range investigated which can be associated to the stiffening effect of the clay. In this case, the presence of C30B in the PE matrix increased storage modulus from 219.9 MPa (neat PE) to 853.9 MPa as can be seen in Figure 3.

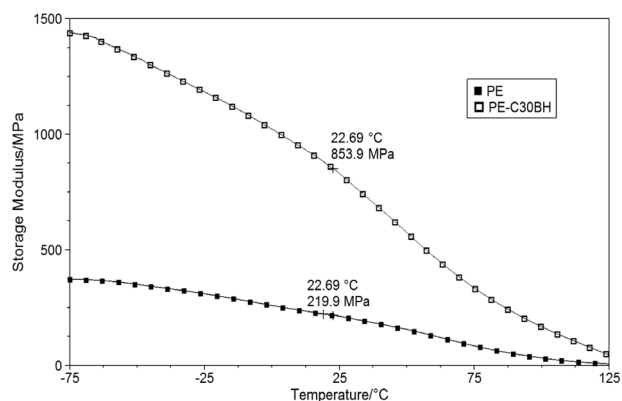


Figure 3. Storage modulus E' for neat PE and PE-C30BH nanocomposite.

Conclusions

We have successfully intercalated **1** into the clay gallery and the resulting catalyst system was able to polymerize ethylene towards the production of PE-MMT nanocomposites. Both XRD and TEM results confirmed the uniform distribution of silicate layers of MMT in the whole PE matrix and the production of exfoliated PE-MMT nanocomposites. Some mechanical properties such as flexural modulus and storage modulus of PE-MMT nanocomposites showed some improvements when compared with those ones displayed by the neat PE produced using exclusively **1**.

Acknowledgments

This work was supported by Braskem S.A and CTPETRO/CNPq (proc. 550145/05-2). Mariana S. Beauvalet, Fernando Junges and Adriana C. A. Casagrande gratefully acknowledge CNPq for the fellowships. The authors thank Braskem S.A for the permission to publish this work.

Reference

- Komori, Y.; Kuroda, K.; *Polymer-Clay Nanocomposites*, Pinnavaia, T. J.; Beall, G. W., eds.; John Wiley and Sons Ltd.: New York, 2001, pp. 3-18.
- Harrats, C.; Groeninckx, G.; *Macromol. Rapid Commun.* **2008**, *29*, 14.
- Gorrasi, G.; Tortora, M.; Vittoria, V.; Kaempfer, D.; Mülhaupt, R. *Polymer* **2003**, *44*, 3679.
- Okada, A.; Usuki, A.; *Macromol. Mater. Eng.* **2006**, *291*, 1449.
- Alexandre, M.; Dubois, Ph.; *Mater. Sci. Eng., R* **2000**, *28*, 1.
- Mariott, W. R.; Chen, E. Y.-X.; *J. Am. Chem. Soc.* **2003**, *125*, 15726.
- Zeng, C.; Lee, L. J.; *Macromolecules* **2001**, *34*, 4098.
- Huskic, M.; Zigon, M.; *Eur. Polym. J.* **2007**, *43*, 4891.
- Paul, M. A.; Alexandre, M.; Degée, P.; Calberg, C.; Jérôme, R.; Dubois, P.; *Macromol. Rapid Commun.* **2003**, *24*, 561.
- Rehab, A.; Akelah, A.; Agag, T.; Shalaby, N.; *Polym. Adv. Technol.* **2007**, *6*, 463.
- Lepoittevin, B.; Pantoustier, N.; Devalckenaere, M.; Alexandre, M.; Kubies, D.; Calberg, C.; *Macromolecules* **2002**, *35*, 8385.
- Liao, L.; Zhang, C.; Gong, S.; *Macromol. Rapid Commun.* **2007**, *28*, 1148.
- Zeng, Q.H.; Wang, D.Z.; Yu, A.B.; Lu, G.Q.; *Nanotechnology* **2002**, *13*, 549.
- Akelah, A.; Rehab, A.; Agag, T.; Betiha, M.; *J. Appl. Polym. Sci.* **2006**, *103*, 3739.
- Essawy, H. A.; Badran, A. S.; Youssef, A. M.; El-Hakim, A. E-F. A. A.; *Macromol. Chem. Phys.* **2004**, *205*, 2366.
- Du, K.; He, A. H.; Liu, X.; Han, C. C.; *Macromol. Rapid Commun.* **2007**, *28*, 2294.
- He, A.; Wang, L.; Li, J.; Dong, J.; Han, C. C.; *Polymer* **2006**, *47*, 1767.
- He, A. H.; Hu, H. Q.; Huang, Y. J.; Dong, J. Y.; Han, C. C.; *Macromol. Rapid Commun.* **2004**, *25*, 2008.
- Sun, T.; Garcés, J. M.; *Adv. Mater.* **2002**, *14*, 128.
- Tudor, J.; Willington, L.; O'Hare, D.; *Chem. Commun.* **1996**, 2031.
- Jongsomjit, B.; Panpranot, J.; Praserttham, P.; *Mater. Lett.* **2007**, *61*, 1376.
- Qian, J.; Guo, C.-Y.; Wang, H.; Hu, Y.; *J. Mater. Sci.* **2007**, *42*, 4350.

23. Malucelli, G.; Ronchetti, S.; Lak, N.; Priola, A.; Dintcheva, N. T.; La Mantia, F. P.; *Eur. Polym J.* **2007**, *43*, 328.
24. Bergman, J. S.; Chen, H.; Giannelis, E. P.; Tomas, M. G.; Coates, G. W.; *Chem. Commun.* **1999**, 2179.
25. Heinemann, J.; Reichert, P.; Thomann, R.; Müllhaupt, R.; *Macromol. Rapid Commun.* **1999**, *20*, 423.
26. He, F.-A.; Zhang, L.-M.; Jiang, H.-L.; Chen, L.-S.; Wu, Q.; Wang, H.-H.; *Compos. Sci. Technol.* **2007**, *67*, 1727.
27. He, F.-A.; Zhang, L.-M.; *Nanotechnology* **2006**, *17*, 5941.
28. Huang, Y.; Yang, K.; Dong, J.-Y.; *Macromol. Rapid Commun.* **2006**, *27*, 1278.
29. Huang, Y.; Yang, K.; Dong, J.-Y.; *Polymer* **2007**, *48*, 4005.
30. Jin, Y.-H.; Park, H.-J.; Im, S.-S.; Kwak, S.-Y.; Kwak, S.; *Macromol. Rapid Commun.* **2002**, *23*, 135.
31. Xu, J.-T.; Zhao, Y.-Q.; Wang, Q.; Fan, Z.-Q.; *Polymer* **2005**, *46*, 11978.
32. Kuo, S.-W.; Huang, W.-J.; Huang, S.-B.; Koa, H.-C.; Chang, F.-C.; *Polymer* **2003**, *44*, 7709.
33. Alexandre, M.; Dubois, Ph.; Sun, T.; Garces, J. M.; Jérôme, R.; *Polymer* **2002**, *43*, 2123.
34. Murtuza, S.; Casagrande, O. L. Jr.; Jordan, R. F.; *Organometallics* **2002**, *21*, 1882.
35. Chiang, R.; *J. Polym. Sci.* **1959**, *36*, 91.
36. Casagrande, O. L. Jr.; Casagrande, A. C. A.; Junges, F.; Beuavalet, M. S.; Barbosa, C. A. S.; Mauler, R. S.; Mota, F. F.; Oviedo, M. A. S.; *Br Patent 0602894-2*, **2006**.
37. Casagrande, O. L. Jr.; Casagrande, A. C. A.; Junges, F.; Beuavalet, Mauler, R. S.; Mota, F. F.; *Br Patent 0605664-4*, **2006**.
38. Fu, X.; Qutubuddin, S.; *Polymer* **2001**, *42*, 807.
39. Zhong, Y.; Zhu, Z.; Wang, S.-Q.; *Polymer* **2005**, *46*, 3006.

Received: September 14, 2008

Web Release Date: February 13, 2009